AD_____
(Leave blank)

Award Number:
W81XWH-05-1-0363

TITLE:
Miniature and molecularly specific optical screening technologies for breast cancer

PRINCIPAL INVESTIGATOR:
Nimmi Ramanujam, Ph.D.

CONTRACTING ORGANIZATION:
Duke University
Durham, NC 27708

REPORT DATE:
October 2010

TYPE OF REPORT:
Annual

PREPARED FOR: U.S. Army Medical Research and Materiel Command
Fort Detrick, Maryland 21702-5012

DISTRIBUTION STATEMENT: (Check one)

X Approved for public release; distribution unlimited

☐ Distribution limited to U.S. Government agencies only; report contains proprietary information

REPORT DOCUMENTATION PAGE

Form Approved
OMB No. 0704-0188

1. REPORT DATE *(DD-MM-YYYY)*	**2. REPORT TYPE**	**3. DATES COVERED** *(From - To)*
01-10-2010	Annual	01 SEP 2009 - 31 AUG 2010

4. TITLE AND SUBTITLE

Miniature and molecularly specific optical screening technologies for breast cancer

5a. CONTRACT NUMBER
W81XWH-05-1-0363

5b. GRANT NUMBER
W81XWH-05-1-0363

5c. PROGRAM ELEMENT NUMBER

6. AUTHOR(S)

Nimmi Ramanujam, Ph.D.

nimmi@duke.edu.

5d. PROJECT NUMBER

5e. TASK NUMBER

5f. WORK UNIT NUMBER

7. PERFORMING ORGANIZATION NAME(S) AND ADDRESS(ES)

Duke University
Biomedical Engineering
136 Hudson Hall
Durham, NC 27708

8. PERFORMING ORGANIZATION REPORT NUMBER

9. SPONSORING / MONITORING AGENCY NAME(S) AND ADDRESS(ES)

U.S. Army Medical Research
Fort Detrick, Maryland 21702-

10. SPONSOR/MONITOR'S ACRONYM(S)

11. SPONSOR/MONITOR'S REPORT NUMBER(S)

12. DISTRIBUTION / AVAILABILITY STATEMENT

Approved for public release; distribution unlimited.

13. SUPPLEMENTARY NOTES

14. ABSTRACT

The goal of this proposal is to harness the power of light to create "miniature and molecularly specific optical technologies" for breast cancer diagnosis and detection. The miniature technologies will leverage on millimeter scale silicon detectors and LEDs to make compact devices that can be used in a practical clinical setting for breast cancer detection. The features that will be exploited for optical detection/diagnosis of breast cancer will include the physiological, structural and molecular alterations that accompany the transformation of a cell from a normal to malignant state. This proposal also focuses on using contrast agents, specifically aminolevulinic acid (ALA) induced protoporphyrin IX (PpIX) and NBDG, for the molecular detection of breast cancer.

15. SUBJECT TERMS

optical, spectroscopy, imaging, fiber-optic, molecular, screening

16. SECURITY CLASSIFICATION OF:			**17. LIMITATION OF ABSTRACT**	**18. NUMBER OF PAGES**	**19a. NAME OF RESPONSIBLE PERSON**
a. REPORT	**b. ABSTRACT**	**c. THIS PAGE**			USAMRMC
U	U	U	UU	22	**19b. TELEPHONE NUMBER** *(include area code)*

Table of Contents

INTRODUCTION	**4**
BODY PROJECT 1	**4**
BODY PROJECT 2	**15**
KEY RESEARCH ACCOMPLISHMENTS	**20**
REPORTABLE OUTCOMES	**20**
CONCLUSIONS	**21**

1. INTRODUCTION

The objective of this proposal is to harness the power of light to create “miniature and molecularly specific optical technologies” for the eradication of breast cancer. Specifically this application focuses on a system on a chip device to detect molecularly specific sources of optical contrast for breast cancer. Both intrinsic (hemoglobin saturation, total hemoglobin content, reduction-oxidation ratio) and extrinsic sources of optical contrast (specifically aminolevulinic acid (ALA) induced protoporphyrin IX (PpIX) and 2-[*N*-(7-nitrobenz-2-oxa-1,3-diazol-4-yl)amino]-2-deoxy-D-glucose (2-NBDG) will be studied for breast cancer imaging. These sources of contrast coupled with the system on a chip device will be initially used for intraoperative margin assessment and predicting/evaluating response to therapy. Once we have established the feasibility of using this technology in the margin assessment and therapy application, we will focus on applications that focus on early detection, including core needle biopsy and ductoscopy, which require further modifications to the technology.

2.1 Body Project 1: System-on-a-chip device

A. Original SOW for five years

1) *To establish the design specifications of the first-generation system-on-a-chip device.* This aim will involve throughput calculations and Monte Carlo modeling to determine the signal-to-noise ratio that can be achieved with the nano scale sources and detectors, and the experimental evaluation of the signal-to-noise of the test system on turbid “tissue-like” media. The signal-to-noise ratios achieved with the test system will be quantitatively compared to that achieved with a standard bench top system (year 1).
2) *To engineer and test the first-generation system-on-a-chip device.* The knowledge base derived from aim 1 will be used to engineer a first generation system-on-a-chip device and the performance of the device will be characterized on synthetic tissue phantom models. The signal-to-noise ratio and fluorescence attenuation characteristics of the system-on-a-chip device will be compared to that of a standard bench top counterpart (year 2).
3) *To experimentally establish the signal-to-noise ratio with which the system-on-a-chip device can measure the fluorescence of ex vivo human breast tissues.* The system-on-a-chip device will be used to measure the fluorescence properties of 25 pair of malignant and non-malignant breast tissues excised from approximately 25 patients undergoing breast cancer surgery. The results obtained from this study will be quantitatively compared to benchmarks established by our bench top counterpart, which has been shown to measure breast tissue fluorescence with excellent signal-to-noise ratio (year 3).
4) *To test the feasibility of implementing optical spectroscopy via a ductoscope.* The system-on-a-chip device will be incorporated into a standard ductoscope. The ductoscope will be used to measure the fluorescence properties of 25 pair of malignant and non-malignant breast tissues excised from approximately 25 patients undergoing breast cancer surgery (years 4-5).

B. Summary of accomplishments in year 1

In year 1, we have completed the main goals of the SOW for year 1. The major achievements include thermal modeling of the heat dissipation effects of compact LEDs on tissue samples,

selection of multi-wavelength compact light sources, calculating bandwidth effects of broadband light sources (such as LEDs) on the RMS errors for the extracted tissue optical and physiological properties, selection of photodiodes, and the design and testing of various single-pixel probe prototypes (P1 and P2 as shown in Figure 2.1). The major deviation from the SOW is that we used commercially available light sources and detector in our design, instead of using nano scale sources.

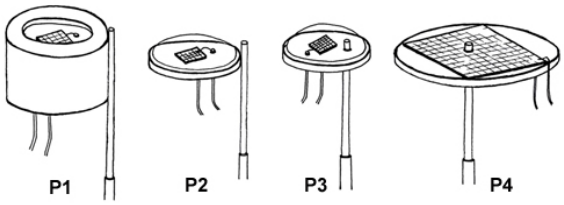

Figure 2.1. Conceptual drawings of four single-pixel probe geometries P1-P4.

C. Summary of accomplishments in year 2

In year 2, we used knowledge base derived from year 1 to build more first generation single-pixel devices using an optical fiber for illumination and photodiodes for the collection of diffusely reflected light from a tissue sample. In particular, we have built single-pixel probes of different illumination and detection geometries named as P3-1 (600 μm fiber), P3-2 (1 mm fiber), P4-1 (600 μm fiber), and P4-2 (1 mm fiber), as shown in Figure 2.1, all using and 2.4 mm photodiode. P3-1 and P3-2 were tested in synthetic tissue phantoms with known optical properties, and their experimental diffuse reflectance spectra were compared with those of a forward Monte Carlo model.

We have also extracted the phantom optical properties from the diffuse reflectance spectra obtained from a tunable light source using an inverse Monte Carlo (MC) model. For P3-2, we found that the overall errors for quantifying the absorption and scattering coefficients were 6.0±5.6% and 6.1±4.7%, respectively. These results are comparable with those achieved with our bench-top system which has an overall error 5.8±5.1% and 3.0±3.1% for extracting μ_a and μ_s', respectively. A short paper on P3-2 has been accepted for publication by the Journal of Biomedical Optics Letters [1] and a copy of the manuscript is attached to this report. Phantom optical properties with reduced number of wavelengths were also extracted and compared to that of the bench-top system with all wavelengths.

In year 2, a clinical study conducted by our group using the bench-top system and the MC model showed that DRS alone has achieved comparable sensitivity and specificity for discriminating malignant from nonmalignant breast tissues as combined reflectance and fluorescence spectroscopy[2]. Therefore, our research in this miniature device has been focused mainly on diffuse reflectance spectroscopy (DRS) for breast cancer diagnosis and tumor margin assessment.

D. Summary of accomplishments in year 3

In year 3, we have modified the probe geometries of the single-pixel probe developed in year 2 in order to increase the signal-to-noise ratio of the probe and to be able to extract a much larger

range of optical properties than those of the probes built in year 2. The new probe was tested in synthetic tissue phantoms over a wide range of absorption and reduced scattering coefficients, and the phantom optical properties were extracted from the diffuse reflectance spectra obtained from the tunable light source and new probe with the inverse MC model previously developed by our group. Using the same phantom data collected by our new probe, optical properties with a reduced number of wavelengths were extracted to assess the feasibility of replacing the tunable light source with several smaller LEDs to further reduce the size and cost of the current system. In addition, cross-talk analysis was performed as a first step to multiplex the single pixel system into an imaging system that can quantify tissue physiological and morphological properties over a large tissue area. We have also fabricated a 3x3 fiber-photodiode array for test in the lab.

Although the original goals of the SOW is to use the system-on-a-chip device to measure the fluorescence properties of 25 pair of malignant and non-malignant breast tissues excised from approximately 25 patients undergoing breast cancer surgery, we understand that many challenges exist and it may take a relatively long time to reach this goal. As an intermediate step, the work in year 3 has been focused on partially miniaturizing the current bench-top system. This miniaturized probe preserves the potential for multiplexing that can be used for spectral imaging of tissue while uses all the wavelengths available to the bench-top system.

In year 3, a poster on the single-pixel device titled “A Miniature Optical Device for Noninvasive, Fast Characterization of Tumor Pathology,” was presented to the 2008 OSA Topic Meeting in Biomedical Optics**,** March 16-19, 2008, St. Petersburg, Florida. A journal paper titled “Cost-effective diffuse reflectance spectroscopy device for quantifying tissue absorption and scattering in vivo,” was also published in Journal of Biomedical Optics Letters in 2008.

E. Summary of accomplishments in year 4

In year 4, the single-pixel probe (using a 5.8x5.8 mm Si detector) with fiber-based illumination developed in year 3 have been expanded to a 3x3 spectral imaging (FISI) array. A FISI system was constructed using the 3x3 array and an 8-wavelength xenon light source. The FISI system was tested in a number of homogeneous liquid phantoms with optical properties representative of breast tissue and excellent accuracy was achieved in extraction of the phantom optical properties. This demonstrated the possibility of performing spectral imaging with low cost photodiodes and 8 LEDs covering the wavelength range from 400 – 600 nm. To further reduce the size and cost and to simplify the probe fabrication, we have proposed a new back-illumination strategy to replace the fiber-based illumination. A single-pixel version of the back-illuminated probe (using a 2.4x2.4 mm Si detector) was built and tested and the performance was found to be comparable to those of the FISI array and the current clinical system. A 4x4 back-illuminated spectral imaging (BISI) array has also been designed and the optimization and testing will be performed in year 5. The drilled commercial Si detectors are good for proof-of-concept study, but our long term goal is to build a system-on-a-chip spectral imaging device, which requires the integration of photodiodes, light delivery network and electronics on to a single wafer. In year 4, we have also made initial GaAs photodiode arrays that will be improved and optimized in year 5.

In year 4, a peer reviewed journal article titled “A strategy for quantitative spectral imaging of tissue absorption and scattering using light emitting diodes and photodiodes” was published in *Optics Express* (Opt Exp 17 (3):1372-1384, 2009). A poster on the 3x3 FISI system titled “A Reduced-Cost Spectral Imaging System for Breast Tumor Margin Assessment," was presented to ECI conference on Advances in Optics for Biotechnology, Medicine, and Surgery XI. Burlington, VT, USA, June 2009.

F. Progress report for year 5

Revised SOW:

Due to the deviation of the SOW for years 1-4, our research plans on the system-on-a-chip for years 5 were also revised accordingly.

- To further investigate the wavelength reduction strategy with bandwidth effects
- To complete development of the 4x4 BISI system.
- To test the 4x4 BISI systems in the imaging mode using Intralipid phantoms.
- To investigate new methods to improve fabrication repeatability of the detector array
- To modify the Monte Carlo model for heterogeneous media

In year 5, we have made significant progress in each of the following areas:

(a) Wavelength Reduction with Bandwidth Effects

In Year 1, we had previously demonstrated via Monte Carlo simulations that we are only able to extract optical properties with < 20% as long as the full-width half-maximum (FWHM) of the chosen center wavelengths does not exceed 30 nm. As we have come closer to being able to implement other illumination sources, such as LEDs, into our system, we have found that some LEDs have FWHM that exceed 30 nm. We have made improvements to our inverse Monte Carlo model of reflectance to take into account the various bandwidths that could affect our optical properties extraction accuracy.

To check the modified Monte Carlo model of reflectance, we simulated 66 different reflectance spectra, which consist of 11 phantoms with varying levels of oxy- and deoxy-hemoglobin concentrations (Total hemoglobin (THb): 1, 4, 10, 15, 20, 25, 30, 35, 40, 45, 50 μM) at 6 varying scattering levels (μ_s': 4.2, 6.1, 10.5, 12.6, 16.9, 18.9 cm^{-1}). To invert the data, we used the same 8 wavelengths of our xenon source from Asahi Spectra that we have previously used: 400, 420, 440, 470, 500, 530, 570, and 600 nm.

Table 2.1 reiterates the need for our Monte Carlo model to take FWHM into account. As the FWHM of the center wavelengths increases, the extraction errors of optical properties also increase. Errors of greater than 40% are obtained when the FWHM is increased past 30 nm, and this is unacceptable for clinical utility as the contrast, for example between malignant and benign tissues, inevitably becomes washed out.

Table 2.1 - Monte Carlo inversion accuracy *without* accounting for bandwidth effect of 8 wavelengths. The diffuse reflectance spectra were simulated using the forward MC model.

	FWHM = 1 nm				FWHM = 5 nm				FWHM = 10 nm			
	μ_a		μ_s'		μ_a		μ_s'		μ_a		μ_s'	
THb	Err (%)	σ	Err (%)	σ	Err (%)	σ	Err (%)	σ	Err (%)	σ	Err (%)	σ
1	0.00	0.00	0.00	0.00	0.75	0.37	0.40	0.26	8.12	7.24	3.93	4.01
4	0.00	0.00	0.00	0.00	0.90	0.40	0.37	0.24	7.84	6.91	3.83	3.80
10	0.00	0.00	0.00	0.00	1.12	1.48	0.30	0.16	7.60	6.99	2.80	3.62
15	0.00	0.00	0.00	0.00	0.81	0.91	0.23	0.13	5.75	5.36	2.56	2.91
20	0.00	0.00	0.00	0.00	0.40	0.23	0.14	0.06	4.21	3.83	1.48	1.52
25	0.00	0.00	0.00	0.00	0.97	1.47	0.20	0.10	5.48	5.25	2.80	3.07
30	0.00	0.00	0.00	0.00	0.63	0.82	0.14	0.07	3.04	2.87	1.27	1.35
35	0.00	0.00	0.00	0.00	1.11	1.74	0.20	0.12	5.19	4.79	2.83	2.77
40	0.00	0.00	0.00	0.00	0.91	1.28	0.19	0.10	2.69	2.18	1.35	1.23
45	0.00	0.00	0.00	0.00	1.13	1.59	0.22	0.12	3.90	3.79	2.32	2.20
50	0.00	0.00	0.00	0.00	1.76	2.96	0.29	0.28	11.88	10.26	4.32	2.67

Table 2.2 shows the Monte Carlo inversion accuracies of our newly improved model, in which the bandwidth effect is accounted for. Using the 8 wavelengths that span between 400 and 600 nm, we are able to accurately extract total hemoglobin concentrations, as well as to differentiate between oxy- and deoxy-hemoglobin concentrations, with essentially 0% error. This is important for the extraction of hemoglobin saturation, which we have found to be a significant parameter in contrasting various breast tissue types and ultimately between cancer and benign tissues.

Table 2.2 - Monte Carlo inversion accuracy *with* bandwidth effect accounted for. The diffuse reflectance spectra were simulated using the forward MC model.

	FWHM = 10 nm				FWHM = 20 nm				FWHM = 30 nm			
	μ_a		μ_s'		μ_a		μ_s'		μ_a		μ_s'	
THb	Err (%)	σ	Err (%)	σ	Err (%)	σ	Err (%)	σ	Err (%)	σ	Err (%)	σ
1	0.00	0.00	0.00	0.00	0.00	0.00	0.00	0.00	0.00	0.00	0.00	0.00
4	0.00	0.00	0.00	0.00	0.00	0.00	0.00	0.00	0.00	0.00	0.00	0.00
10	0.00	0.00	0.00	0.00	0.00	0.00	0.00	0.00	0.00	0.00	0.00	0.00
15	0.00	0.00	0.00	0.00	0.00	0.00	0.00	0.00	0.00	0.00	0.00	0.00
20	0.00	0.00	0.00	0.00	0.00	0.00	0.00	0.00	0.00	0.00	0.00	0.00
25	0.00	0.00	0.00	0.00	0.00	0.00	0.00	0.00	0.00	0.00	0.00	0.00
30	0.00	0.00	0.00	0.00	0.00	0.00	0.00	0.00	0.00	0.00	0.00	0.00

35	0.00	0.00	0.00	0.00	0.00	0.00	0.00	0.00	0.00	0.00	0.00	0.00
40	0.00	0.00	0.00	0.00	0.00	0.00	0.00	0.00	0.00	0.00	0.00	0.00
45	0.00	0.00	0.00	0.00	0.00	0.00	0.00	0.00	0.00	0.00	0.00	0.00
50	0.00	0.00	0.00	0.00	0.00	0.00	0.00	0.00	0.00	0.00	0.00	0.00

The improvements in our Monte Carlo model allow us to accurate simulate and track photon paths in turbid media. As we continue to work towards a more complete and cost-effective spectroscopic imaging system, we will inevitably replace an expensive, sophisticated light source which may include monochromators or filter wheels, with LEDs, which can have a variety of bandpasses that differ in shape and width. We will now be able to characterize these shapes and widths of the bandpassses and eliminate them as a source of error in the model.

Furthermore, as shown in Table 2.3, we can also reduce the number of wavelengths required to obtain accurate extractions. We had previously chosen wavelengths that span the 400-600 nm range because of the prominent features of oxy and deoxy-hemoglobin that exist within the range, such as the Soret band around 420, and the alpha and beta bands around 540-580 nm. Table 2.3 shows the importance of the Soret band, which is highly absorbing, for our extraction accuracy as the FWHM is increased. Since the differences between the alpha and beta bands are smaller than the FWHM, the contrast cannot be extracted. In future iterations of the device development, we will implement wavelengths in the 400-500 range to capture the red-shift of deoxy-hemolgobin at the Soret band. In fact, with 2 species of absorbers (oxy- and deoxy-hemoglobin) that overlap in the alpha and beta bands once the FWHM blurs their differences, the extraction errors are increased significantly.

Table 2.3 - Monte Carlo inversion accuracy using different wavelengths at FWHM = 20 nm. The diffuse reflectance spectra were simulated using the forward MC model.

	λ: 470, 500, 530, 570, 600				λ: 440, 470, 500, 530, 570				λ: 400, 420, 440, 470, 500			
	μ_a		μ_s'		μ_a		μ_s'		μ_a		μ_s'	
THb	Err (%)	σ	Err (%)	σ	Err (%)	σ	Err (%)	σ	Err (%)	σ	Err (%)	σ
1	41.78	64.91	5.28	2.00	6.17	6.06	2.70	2.52	0.02	0.18	0.01	0.08
4	41.03	63.79	5.39	2.11	6.16	6.43	2.60	2.34	0.00	0.00	0.00	0.00
10	38.89	62.49	5.35	2.21	5.84	6.01	2.44	2.18	0.00	0.00	0.00	0.00
15	42.89	74.45	5.39	2.17	5.93	5.77	2.55	2.21	0.00	0.00	0.00	0.00
20	42.03	67.51	5.35	1.96	5.68	5.66	2.44	2.11	0.00	0.00	0.00	0.00
25	41.06	67.54	5.19	2.07	5.99	6.06	2.50	2.19	0.00	0.00	0.00	0.00
30	40.87	64.02	5.27	2.07	5.77	5.69	2.52	2.18	0.00	0.00	0.00	0.00
35	40.88	63.84	5.35	1.98	6.26	6.54	2.61	2.26	0.02	0.19	0.01	0.08
40	40.42	64.18	5.29	2.26	5.54	5.96	2.31	2.00	0.00	0.00	0.00	0.00
45	42.15	70.21	5.24	2.24	6.09	6.38	2.58	2.36	0.00	0.00	0.00	0.00
50	40.91	64.26	5.20	2.02	6.28	6.00	2.7	2.36	0.00	0.00	0.00	0.00

(b) 4x4 Back-illumination Probe

In Year 4, we showed that we are capable of experimentally extracting optical properties with high accuracy using a single-pixel version of this "back-illumination" strategy in which 8 wavelengths of light is launched from the back, through a hole in the center of a photodiode. We have created a probe with 16 pixels arranged in a 4x4 two-dimensional array as shown in our previous progress report.

In year 5, we characterized the throughput metrics of an initial two-dimensional array of photodiodes and found that the corner pixels have much lower illumination power than the center pixels. For instance, the corner pixels have only a power output of less than 10 μW at 400 nm. By comparison, our single-pixel probe, which we have used to measure and extract optical properties had high accuracies, had a power of more than 40 μW at 400 nm. To alleviate the problems with throughput, we made the holes of the corner pixels slightly larger than the holes of the other pixels (1.25 mm diameter vs. 1.00 mm diameter) to allow more light to pass through. We were then able to get higher throughput from corner pixels; however, this came at the expense of decreasing the size of the photodiode active area, and thus the signal of the corner pixels. We will discuss plans that we have implemented to solve this problem in the subsequent section of this report. Here, we discuss the proof-of-concept of a compact spectroscopic imaging probe that can be used to quantitatively measure optical properties and thus various characteristics of tissue.

To show the idea of spectroscopic imaging with this probe despite the throughput issues we had at the time, we filled four glass capillary tubes with hemoglobin solution and arranged them in a Petri dish as shown in Figure 2.2(a). The Petri dish was filled with 20% intralipid to achieve scattering properties similar to that of breast tissue, average (400-600 nm) μ_s' = 10 cm^{-1}. Diffuse reflectance measurements were made by placing the probe in contact with the liquid surface, with the hemoglobin capillary tubes directly under some of the photodiodes, as shown in Figure 2.2. Inverse Monte Carlo model of reflectance was used to extract optical properties under each pixel. Although we have not, at this point in time, been able to successfully extract optical properties with very high accuracies using the 4x4 detector array, we are still able to see the contrast between pixels with hemoglobin tubes and those without, as shown in Figure 2.2(b). From this figure, there is clearly some contrast between the detectors of row 3 and other rows. With no hemoglobin tubes directly below the detectors in the measurement, the extracted μ_a is low, and thus Hb is also close to 0. We also expected row 2 to have much higher Hb extraction because there were 2 Hb capillary tubes below those pixels, and the extracted map also shows this. The problem, again, lies in the corner pixels. The signal is low, and thus impacts the accuracies of the extractions. Nonetheless, we are able to show some proof-of-concept imaging *qualitatively* and are still working towards quantitative spectroscopic imaging.

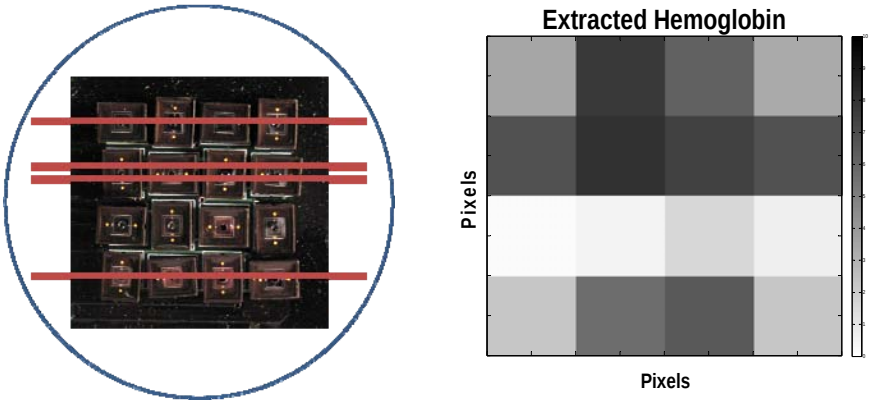

(a) (b)

Figure 2.2. 4x4 BISI system: (a) Schematic of Hb-filled capillary tubes and their arrangement corresponding with 4x4 photodiode locations; (b) Extracted hemoglobin using the 4x4 two-dimensional array of photodiodes

(c) New Array Approach: Lithographically-defined Apertures

The previous 4x4 back-illuminated two-dimensional array had various problems. Because the apertures were mechanically drilled holes, none of the 16 pixels were identical. Furthermore, the mechanical drilling of photodiodes prevents us from accurately modeling the probe geometry, which is very important for our Monte Carlo model. While it was possible to optimize the probe geometry for a single pixel, it became very time-consuming and not practical for 16 or more pixels. We have come up with a new approach that will not only improve the power output of the corner pixels, but also help us to create a very uniform two-dimensional array of detectors.

Instead of trying to fabricate an expensive GaAs detector array, the availability of commercial photodiode dies allows for the formation of multi-pixel arrays with high performance at a reduced cost. Commercial diodes are available which have high performance, typically at the limits of the materials system, are readily available and are low cost per pixel. We have been investigating this approach computationally as well as experimentally. The photodiode dies can be placed with a high degree of accuracy using a novel Si template or mask layer. Since Si can be readily and controllably etched, a silicon wafer can serve several purposes in this application which improves the metrology of the array.

The new array approach consists of a three-layer mask and layer process, as shown in Figure 2.3. The bottom layer consists of a large area transparent silica wafer. Apertures are lithographically defined in a highly reflective gold layer. This silica layer serve to provide a continuous liquid seal against the probed tissue while the gold layer serves and a common backside ground plane for the photodiodes. A second layer consists of a silicon wafer which is through etched to provide both an aligned aperture to the underlying silica layer and a highly registered frame to surround and hold the photodiode die. This silicon wafer layer is oxidized which provides an insulating layer enabling electrical isolation of each photodiode. The final layer consists of lithographically defined gold wiring tracks. The assembly consists of aligning the apertures in the silica and silicon. The two aligned layers are affixed using highly conductive silver-based epoxy. The photodiodes placed and affixed into the close-fitting sockets etched into the silicon wafer. The final steps is wire-bonding the emitters of the photodiodes to the wiring tracks. The entire assembly would eventually be encased in a transparent resin for sealing. Figures 2.4 illustrates this in more detail.

Lithographically defined apertures allow for uniformity. The addition of slits without drilling detectors allow more light to go through to interact with the sample and without decreasing the total active area of the detectors. Furthermore, and perhaps most important of all, the detectors are not damaged at all by any mechanical force, and the probe geometry can be very accurately modeled.

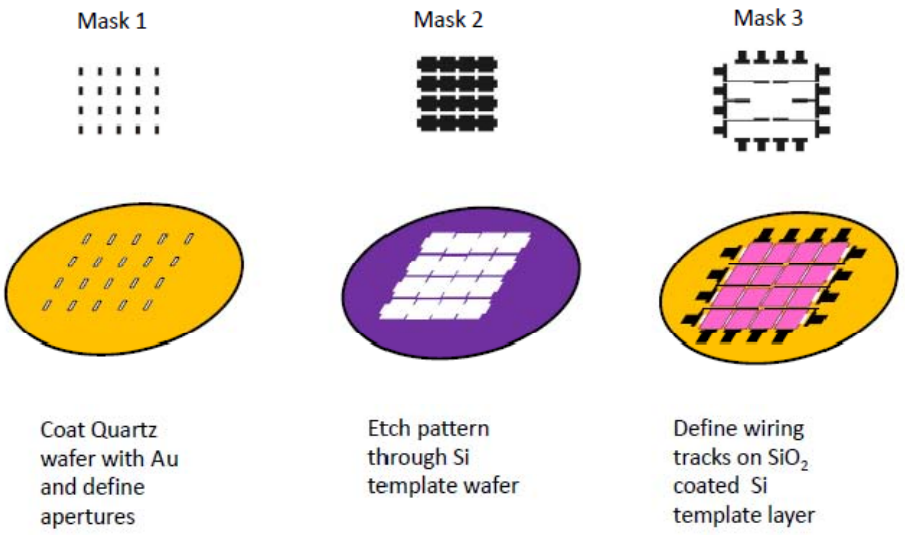

Figure 2.3. Lithographic patterns for the array assembly

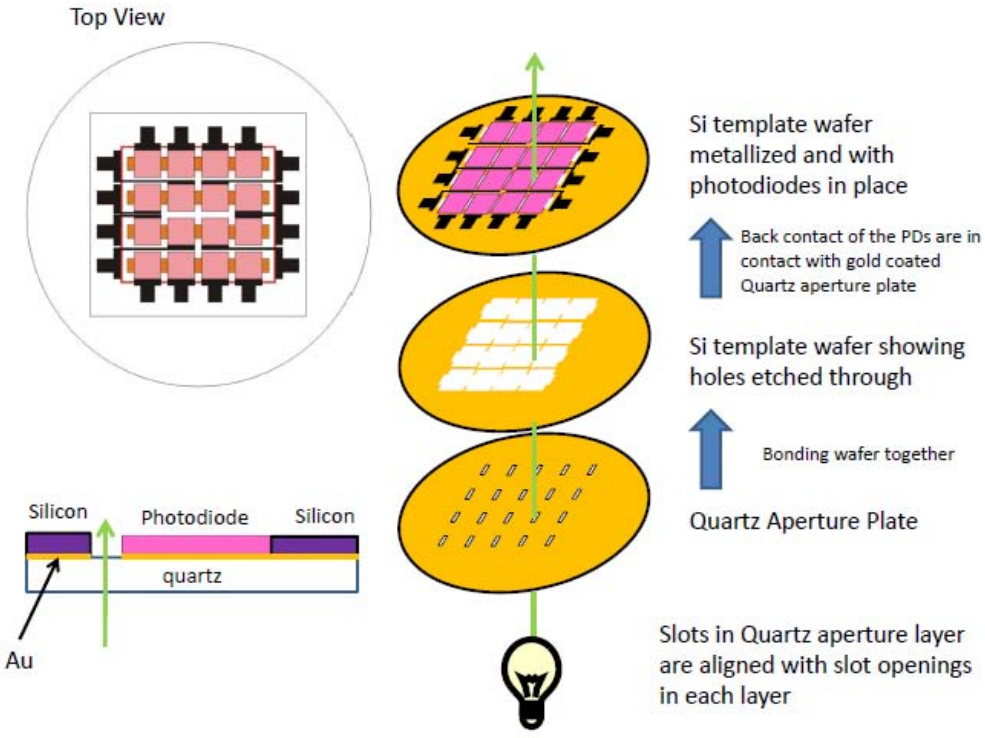

Figure 2.4. Exploded diagram of the assembly and aligned of the layers.

(d) Heterogeneous Monte Carlo Model

The results of the various iterations of the compact spectral imaging devices have demonstrated the ability to quantitatively extract optical properties simultaneously from different regions of a target. Currently the optical property extraction method relies on the important assumption that each individual pixel must be treated independently.

To physically implement this, each pixel of the imaging array must be spaced sufficiently so that light originating at an adjacent pixel's illumination fiber will not be collected. With this restriction in place, each pixel will function properly as an independent unit and the optical properties for each region underneath each pixel can be extracted separately. In order for this assumption to hold valid, the spacing between pixels must be large enough to avoid cross-talk between pixels (~10 mm). This spacing designates the spatial resolution of the system. In order to improve the spatial resolution, the pixel spacing must be reduced. However, if the pixel spacing is reduced even further, cross-talk will become a factor and our current model and assumptions would not be valid.

One of the tasks during the past year of funding was to being developing an algorithm capable of accounting for multiple pixels. Successful development of such a model would enable us to reduce the pixel spacing and significantly improve the spatial resolution. Briefly, Monte Carlo modeling of light transport is the basis of our current model which extracts the optical properties (absorption, μ_a, and scattering, μ_s', coefficients) given a measured diffuse reflectance spectra. Monte Carlo is a method which simulates photons propagating through tissue as they undergo absorption and/or scattering. The path length at which photons are either absorbed or scattered are dictated by the optical properties Again, our current model assumes that the tissue is homogeneous, so only one set of optical properties which are taken into account.

However, once the pixel spacing is reduced and the illumination and detection from adjacent pixels are moved closer together, cross talk between pixels is expected. Regions underneath different pixels may have different optical properties, so this must be taken into account. The first step toward this model development is designing a light transport model using a simple case of a single illumination fiber. However, rather than having a single set of optical properties, the code should allow for multiple regions with different optical properties

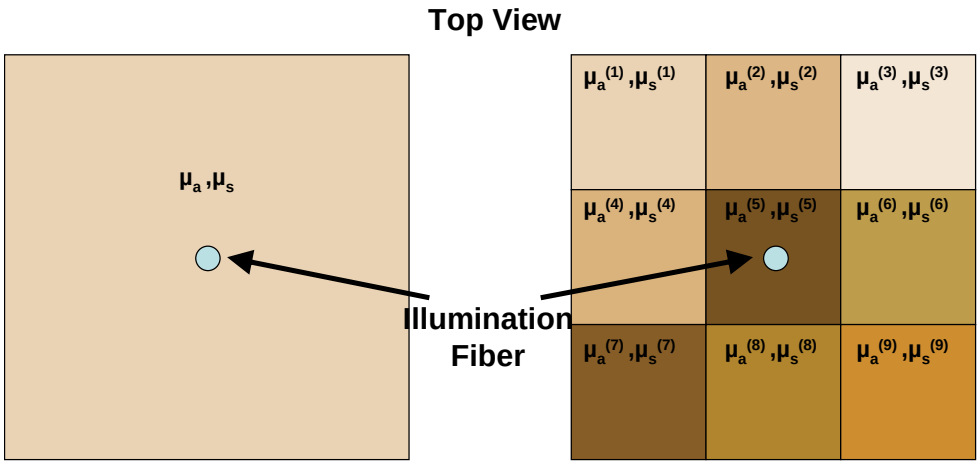

Figure 2.5. Schematics detailing the difference between the homogeneous and heterogeneous light propagation code. Light is launched from the central illumination fiber and allowed to propagate through the multi-region target.

Currently the model is still in the developmental stages, however, the preliminary results and functionality show promise. The design depicted in Figure 2.5 is fully implemented in our current generation of the code. Photons are launched from a central illumination fiber with a diameter as an input parameter. The number of regions, size of each region, and optical properties of each region are also input parameters. The model will simulate photons propagating through the heterogeneous media and track the photons which escape the media. This model represents the forward simulation, given a set of optical properties, the reflectance (escaping photons) can be simulated. The eventual goal of the model is to extract an unknown optical property value given a measured reflectance. Assembling this working forward model is an important initial step. Over the next year we will continue to develop a full heterogeneous Monte Carlo model capable of significantly improving our compact spectral imaging design.

G. Plans for years 6

- To test the single-pixel back-illuminated probe on five ex vivo biological samples
- To build and characterize the new 4x4 BISI detector array
- To test the new 4x4 BISI system in tissue phantoms and five ex vivo biological samples
- To validate the heterogeneous MC model in tissue phantoms

3.1 Body Project 2: **Exploiting, physiological, metabolic and molecular contrast in breast cancer**

A. Original SOW for five years

1) *Physiological and metabolic characterization of mammary tumors in an animal model of breast cancer.* Nude mice will be injected in the flank with 500,000 4T1/D2 cancer cells. The tumors will be allowed to grow until they have reached a size of approximately 8 mm in diameter (approximately 1-2 weeks). Non-invasive optical measurements of tumor oxygenation, vascularity and metabolism will be measured using a continuous wave system and compared to independent measurements of tumor hypoxia using an OxyLite fiber optic sensor and immunohistochemistry of hypoxic and metabolic markers (year 1).

2) *Synthesis of contrast agents for molecular imaging.* Gold nanoparticles will be prepared via citrate reduction of chloroauric acid. The particle size will be adjusted to preferentially scatter NIR light. Anti-HER2 and anti-EGFR antibodies will be conjugated to the gold. The scattering spectrum of (1) the pre-labeled nanoparticles will be measured to verify their NIR resonant scattering properties and (2) the labeled nanoparticles to verify binding with the antibodies (a characteristic red-shift in the peak is expected to occur after binding) (year 2).

3) *Molecular imaging in cells*. Human breast cancer cell lines, MDA-MB-468 and SK-BR-3 which over express EGFR and HER2, respectively will be cultured to test the targeting strategies. Cell lines that express low levels of EGFR and HER2 will be used as controls. Each cell type will be labeled according to previously established protocols and imaged using a microscope coupled to a CCD camera. The optical contrast in the cells over expressing HER2 and EGFR receptors relative to that in the control cells will be statistically compared to demonstrate the molecular specificity of the anti-EGFR and anti-HER2 nanoparticles (year 3).

4) *Molecular imaging in animal models.* Tumor cell lines will be stably transfected to over express both HER2 and EGFR, and tumors will be grown in the mammary fat pad of the nude mice used in (a). Both topical and systemic injection of the molecular contrast agents will be explored. An optical imaging system consisting of a tunable laser and a CCD camera will be used to image the molecularly tagged contrast agents for different doses (to measure the effect of dosimetry on the signal to background) as well as for topical vs. systemic delivery. Note that task (a) is directly relevant to this aim as it will provide the instrumentation and algorithms for data analysis as well as experience with the preparation of animal tumor models for these studies (years 4-5).

The original project proposed here has evolved into two distinct projects: (1) The development of techniques to exploit the intrinsic sources of optical contrast (physiologic and morphological) as a means to assess response to cancer therapy and (2) the assessment of extrinsic sources of optical contrast for use as an aid in intra-operative assessment of breast tumor margins.

B. Summary of Accomplishments in years 1 and 2

The goal of this year 1 study was to quantify and track changes in oxygenation in response to carbogen breathing in 4T1 breast tumors in nude mice using optical spectroscopy. Specifically we measured hemoglobin saturation and the optical redox ratio and compared the optical measures of oxygenation to that of a well established method of measuring tumor pO_2, the OxyLite system, to demonstrate the utility of optical spectroscopy to quantitatively monitor tumor physiology in a pre-clinical model.Non-invasive optical spectroscopy was performed on 4T1

breast tumors grown in the flank of nude mice (n=10) before and after the administration of carbogen (95% O2, 5% CO2), by placing a fiber optic probe in contact with the surface of the tumor.

This work established the ability of optical spectroscopy to consistently track changes in tumor physiology in response to a perturbation. It was found that optical spectroscopy may in fact provide a more robust assessment of tissue oxygenation than the existing Oxylite system, likely due to its larger probing volume. This work establishes optical spectroscopy as a viable tool to monitor changes in tumor physiology in response to other treatments, including radiation, chemotherapy, and molecular therapies, offering many advantages over existing technologies. In particular, it is fast, non-invasive, quantitative, and probes a wide range of physiologic parameters, including blood content, oxygenation, and cellular metabolism. This project has subsequently expanded and will span the full five years of the proposal.

C. Summary of Accomplishments in year 3

Establishing the validity of intrinsic optical biomarkers to quantitatively and longitudinally monitor tumor hypoxia and necrosis in murine tumor models:

Diffuse reflectance spectroscopy was evaluated as a objective tool to assess quantitative physiological changes in solid murine tumor models when exposed to chemotherapy. Specifically, it was investigated whether the optical technique could assess changes in tumor hypoxia and necrosis relative to the traditional immunohistochemical methods. N=50 nude mice were inoculated with 4T1 mouse breast carcinoma cells on their flanks and were evenly distributed into control and treatment groups (each group had 25 animals). The treatment group received an 10 mg/kg of Doxorubicin while the control group received an equivalent volume of saline. The tumors were monitored optically prior to treatment and then for 2 weeks post treatment. Five randomly chosen animals, from each group, were removed for immunohistochemical (IHC) analysis on 4 different days. We found that the optical markers of de-oxygenated hemoglobin and the wavelength-averaged optical tissue scattering coefficient were directly correlated to immunohistochemical assessment of tumor hypoxia and histologically estimated tumor necrosis, respectively. Further we established that the temporal trends in these optical and immunohistochemical parameters were concordant with one another. Another result from this study was that optical measurements indicated a clear and statistically significant increase in the oxygen content in the treated tumors relative to the untreated animals, while both immunohistochemical and tumor growth delay assays showed no differences between the treatment and control groups, lending further credence to the fact that such non-invasive methods may provide both better and earlier indications of treatment effects.

Molecular imaging with 5-ALA:

The research goals for year 3 have changed from the synthesis of scattering contrast agents that was originally proposed to detecting mammary cancer with fluorescent contrast agents. Fluorescence agents were chosen over scattering contrast agents because fluorescence has a unique excitation and emission. In the previous year, aminolevulinic acid (ALA) induced protoporphyrin IX (PpIX) was successfully used to differentiate cancerous cells from normal with

fluorescence lifetime. This work was carried on into the beginning of this year by examining fluorescence intensity and spectroscopy. It was found that PpIX has a significantly greater fluorescence increase in malignant cells as compared to normal cells. However, the raw fluorescence intensity of cells cannot be used to delineate malignant from normal without a fluorescence control to determine the endogenous fluorescence. The long incubation time, 2 hours, and endogenous fluorescence required to detect PpIX is clinically prohibitive. It was concluded that for clinical use within the operating room, PpIX is not ideal.

D. Progress Report for year 4

Using optical spectroscopy to assess early response to radiotherapy using intrinsic optical biomarkers

Introduction: The currently accepted standard practice to assess the efficacy of anti-cancer treatments in preclinical studies uses the tumor growth delay assay. Though useful, the uni-dimensional measurements of tumor volume hide a plethora of functional, physiological and metabolic information regarding how the tumors are responding toward treatments. Further, relying solely on tumor growth/recurrence to indicate treatment response requires a long period of sustained observations. We wanted to evaluate if diffuse reflectance spectroscopy could be used as an objective tool to assess early response in solid murine tumors model that were exposed to radiotherapy. The non-invasive and quantitative nature of this technique along with its ability to performed using a variety of different fiber-optic probe geometries makes it highly relevant to translational applications. We have completed a preliminary animal study to explore the feasibility of using optical biomarkers obtained early during a course of curative radiotherapy in predicting long term local tumor control.

Study Design: N=34 nude mice were inoculated with 10^6 FaDu human hypopharyngeal squamous cell carcinoma cells, subcutaneously, on their right flanks. Once the average tumor diameters reached 6-8 mm, the animals were evenly distributed by tumor volume into control and treatment groups in a 1:2 ratio, respectively. N=23 animals in the treatment group were exposed to 39 Gy of radiation, while N=11 animals in the control group received sham irradiation. The dose of 39 Gy was chosen as it has previously been reported as the TCD_{50} (dose which provides local control to 50% of the treated population) for this tumor model in nude mice. Treatment day was labeled day 0. All tumors were monitored optically before treatment to get baseline measurements on day 0 and then again on days 1, 3, 5, 7, 10, 12, 14 and 17. Tumor volumes were measured once using calipers each day over the course of the optical measurements and then one or two times per week until 120 days post treatment.

Results: This study was one of the first of its kind to demonstrate the predictive ability of a non-invasive sensing method to select animals that had complete local control relative to animals that fail treatment. We observed that animals showing complete local control (as defined by the lack of a palpable/visible lesion 120 days post treatment) showed statistically significant rates of increase in tumor oxygen saturation as early as 7 days post-irradiation, relative to the subjects that failed treatment. These responding animals also maintained higher levels of tumor oxygen saturation relative to the animals that failed treatment up to 17 days post-treatment. We have been able to build preliminary linear discriminant models that were

able to separate the animals that responded to the treatment vs. not with 100% sensitivity and 85% specifity.

Molecular imaging with NBDG

The research goals for year 4 have changed from the original statement of work, synthesis of scattering contrast agents to utilizing metabolic fluorescent contrast agents. Metabolic agents allow for functional imaging of cellular processes and can determine tissue response to therapy. In the previous year, 2-[*N*-(7-nitrobenz-2-oxa-1,3-diazol-4-yl)amino]-2-deoxy-D-glucose, 2-NBDG was used to determine if different receptor statuses in 10 various lines of breast cancer effected uptake. It was found that 2-NBDG has a significantly greater fluorescence increase in breast cancer cells as compared to human mammary epithelial cells (HMEC). It was further determined that glucose transporter (GLUT 1) protein was necessary for uptake of 2-NBDG via Western blot analysis. 2-NBDG uptake was measured in response to anti-cancer therapies lonidamine (LND) and alpha-hydroxycinnamate (a-Cinn). LND directly inhibits HK and was shown to prevent 2-NBDG uptake. A-Cinn prevents cells from transporting lactate across the cellular membrane to use it as a secondary source of energy. This increases the need for glucose and was found to cause an increase in 2-NBDG. It was concluded that glycolytic need could be measured using 2-NBDG.

Progress for year 5:

Introduction: In the previous year, 2-NBDG was shown to be ubiquitously applicable to multiple types of breast cancer. 2-NBDG is a fluorescent glucose analog and accumulates in cancerous cells that have high rates of glycolysis and rely on glucose for energy more than normal cells. We have shown that without GLUT transporters, 2-NBDG will not diffuse across the cellular membrane as with the previously tested HMEC cells. 2-NBDG is excited between 400-500 nm and emits at 540 nm making it ideal for high throughput cellular testing. In year 5 our studies examined whether 2-NBDG can be used to determine cellular treatment responders from non-responders after endocrine therapy. First, the efficacy of the therapy was determined, then molecular glycolytic proteins were measured and finally 2-NBDG uptake. Protein analysis requires cell collection and destruction whereas 2-NBDG measurements can be completed non-invasively with fluorescence microscopy.

Study Design: Tamoxifen, a common endocrine therapy used in breast cancer, is used as an anti-estrogen therapy that prevents esterogen from being effectively used by cells for growth. Estrogen receptor positive cells require estrogen to survive, but normal cells and estrogen receptor negative cells are unaffected. Eight plates of estrogen positive (MCF7) and estrogen negative (MDA-MB-435) cells were treated with 2 μM tamoxifen for 72 hours or a vehicle control. Tamoxifen has previously been shown to decrease the number of GLUT 1 receptors within responsive cells and should decrease the ability to take up 2-NBDG. To determine that the tamoxifen treatment was effective, cell cycle analysis was completed and the relative protein expression of GLUT 1 was determined following Western blot analysis. After treatment, cells were incubated with 200 uM of 2-NBDG in glucose free media. Fluorescence intensity was measured on a Leica SP5 confocal microscope and quantified in ImageJ to determine the fluorescence intensity in cells treated with tamoxifen and those treated with the vehicle control.

Results: The cell cycle analysis determined that 2 μM tamoxifen treatment for 72 hours was effective in MCF7 cells (responders) but not the MDA-MB-435 (non-responders). The Western blot analysis further verified this information by showing a lower GLUT 1 expression in treated MCF7 cells versus vehicle control and no significant difference in treated and vehicle control MDA-MB-435 cells. Quantification of 2-NBDG fluorescence intensity showed that Tam treated MCF7 cells were significantly less fluorescent than vehicle control MCF7 cells. MDA-MB-435 cells did not show a significant difference in 2-NBDG uptake in the tam treated and vehicle control.

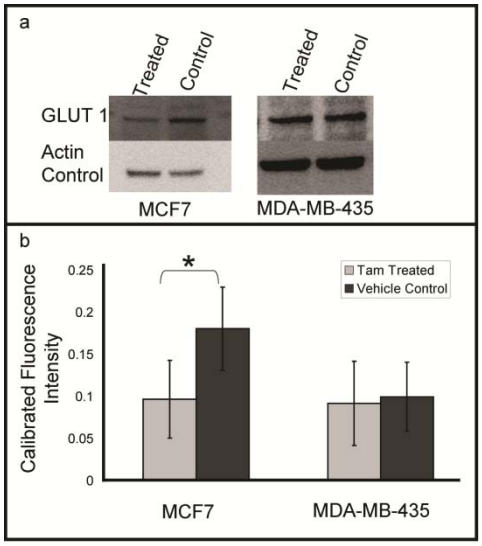

Figure 3.1 shows the Western blot analysis of GLUT 1 expression and actin as an internal control (a) and mean and standard deviation of the fluorescence intensity of treated and vehicle control cells (b).

These tests demonstrate that 2-NBDG has potential to be exploited for high throughput cellular analysis of drug candidates. A decrease in the baseline level of GLUT 1 after tamoxifen treatment directly decreased 2-NBDG uptake. In these studies, 2-NBDG was able to delineate responder cells from non-responder cells.

Plans for year 6: In Year 6, we will employ the use of a murine model to evaluate the distribution of 2-NBDG within a tumor. The 4T1-RFP (red fluorescent protein) mouse mammary tumor line will be implanted in mice to determine whether 2-NBDG can be used to visualize the distribution of 2-NBDG throughout a tumor as well as the hemoglobin saturation of the tumor tissue to be able to compare uptake and vasculature. This will be potentially be examined real-time on an *in vivo* hyperspectral microscope with a window chamber model and/or in a flank tumor using point-based spectroscopy.

3. KEY RESEARCH ACCOMPLISHMENTS

Project 1. System-on-a-chip device

- We have modified the Monte Carlo inverse model to account for reduced number of wavelength and bandwidth effects.
- We experimentally characterize the throughput and SNR of the 4x4 back-illuminated imaging array and partially improved the throughput for the corner pixels.
- We have tested the 4x4 BISI array for spectral imaging using Intralipid phantoms with hemoglobin capillary tubes to simulate heterogeneous biological tissue.
- A new design has been proposed to improve fabrication repeatability of the detector array.
- We have also modified the Monte Carlo model for heterogeneous media

Project 2. Exploiting, physiological, metabolic and molecular contrast in breast cancer

- Longitudinal measurements of tumor physiology using optical biomarkers provide early estimates of changes in tumor oxygenation patterns in irradiated tumors.
- Rapid and sustained reoxygenation in irradiated tumors indicates better probability for long term local tumor control in irradiated tumors.
- Optical biomarkers may be able to predict long-term treatment outcomes as early as 1-2 weeks after treatment initiation.
- In the previous year, 2-NBDG was not linearly correlated with overall GLUT 1 expression, but activity. In this year of research we have shown that direct decreases in GLUT 1 cause a decrease in 2-NBDG uptake.
- 2-NBDG was used to delineate cellular responders from non-responders to endocrine breast therapy.

4. REPORTABLE OUTCOMES

Project 1. System-on-a-chip device

1) Lo JY, Yu B, Fu HL, Bender JE, Palmer GM, Kuech TF, Ramanujam N. "A strategy for quantitative spectral imaging of tissue absorption and scattering using light emitting diodes and photodiodes." *Optics Express*. 17 (3):1372-1384, 2009.

2) H.L. Fu, B. Yu, J.Y. Lo, T.F. Kuech, and N. Ramanujam, “A Low Cost System for Quantitative Spectral Imaging of Tissue Absorption and Scattering,” ECI Conference on Advances in Optics for Biotechnology, Medicine and Surgery XI *Clinical Challenges and Research Solutions,* June 28 - July 2, 2009, Burlington, Vermont, USA.

3) Fu HL, Yu B, Lo JY, Palmer GM, Kuech TF, Ramanujam N, "A Cost-Effective, Portable, and Quantitative Spectral Imaging System for Application to Biological Tissues" Optics Express, Vol. 18, Issue 12, pp. 12630-12645 (2010).

Project 2. Exploiting, physiological, metabolic and molecular contrast in breast cancer

1) Millon SR, Ostrander JH, Brown JQ, Ramanujam N. "Uptake of 2-NBDG in normal mammary epithelial and breast cancer cells." ECI (2009).

2) Millon SR, Ostrander JH, Brown JQ, Ramanujam N. "2-NBDG for use in breast cancer detection and therapy monitoring in vitro." Fitzpatrick Symposium: Frontiers in Photonics and Science (2009).

3) Millon SR, Ostrander JH, Brown JQ, Ramanujam N. "2-NBDG for use in breast cancer detection and therapy monitoring in vitro." Duke Comprehensive Cancer Center Annual Meeting. (2009).

4) Vishwanath K, Huan Y, Barry WT, Dewhirst MW, and Ramanujam N. Using Optical Spectroscopy to Longitudinally Monitor Physiological Changes within Solid Tumors. *Neoplasia* **11**, 889-900. 2009

5) Vishwanath K, Klein D, Chang K, Schroder T, Dewhirst M, and Ramanujam N. Quantitative optical spectroscopy can identify long term local control in irradiated murine head and neck xenografts. *J Biomed Opt* 14(5), 054051. 2009

6) Millon SR, Ostrander JH, Brown JQ, Rajeha AM, Seewaldt VL, Ramanujam N. "Uptake of 2-NBDG as a method to monitor therapy response in breast cancer cell lines." Breast Cancer Research and Treatment. (2010). In Print.

5. CONCLUSIONS

A. Project 1. System-on-a-chip device

In year 5, we have modified the Monte Carlo inverse model for reflectance to account for reduced number of wavelength and bandwidth effects. This improved MC model will enable us to replace the expensive Xe light source with a filter wheel with a handful of low-cost LEDs, making is possible to build a very compact quantitative spectral imaging device that can be used for intra-operative tumor margin assessment. Our phantom experiments with the 4x4 BISI array indicated that it is feasible to perform quantitative imaging of heterogeneous samples with the device, but the throughput, illumination uniformity, and fabrication processes need to further improvement for better accuracy and repeatability. We hope the new design of the 4x4 array will help us to achieve these goals in the no cost extension year (year 6). In the meantime, we have also modified the Monte Carlo model of reflectance for heterogeneous media, which will allow us to simulate imaging arrays with significant crosstalk among adjacent pixels and thus improving the spatial resolution of the device.

A. Project 2

a. Molecular imaging with NBDG

In the previous year, a large panel of breast cancer cell lines of varying receptor types and normal mammary epithelial cells were tested to determine whether 2-NBDG could be used to delineate endocrine therapy responders from non-responders. Two cell lines (a responder and non-responder) were treated with tamoxifen. Tamoxifen efficacy was verified via cell cycle

analysis and molecular expression of the GLUT 1 receptor was quantified. Tamoxifen decreased the GLUT 1 receptor expression in responder cells. Fluorescence intensity was then used to determine the differences in 2-NBDG uptake. 2-NBDG uptake was found to be significantly reduced in responder cells ($p<0.01$). This demonstrates potential of 2-NBDG as a non-invasive method to monitor cellular response to therapy.

b. Assessing treatment outcome using optical spectroscopy

In year 4, we specifically tested whether a sequence of longitudinal optical spectroscopic measurements obtained for up to two weeks post-radiotherapy could predict for long term loco-regional control in one human squamous cell carcinoma cell line, in a nude mouse model. The results from this preliminary study established (a) that optical spectroscopy can provide a useful, non-invasive and simple means to monitor perturbations in tumor physiology as a function of treatment, (b) that there were significant differences in the patterns of tumor oxygenation following treatment in individual subjects, and (c) that the trends in tumor oxygenation could statistically significantly ($p < 0.01$) discriminate between animals that showed local control vs. those that failed treatment, as early as 7 days post treatment. We intend to further explore the validity of optical methods in predicting early treatment response to radiotherapy in future studies by: (i) using a fractionated radiation treatment schedule to better reflect clinically followed treatment schedules, and (ii) testing additional cancer cell lines.